

論文 / 著書情報
Article / Book Information

論題(和文)	
Title(English)	Effects of Wind Characteristics on Residual Drift of the Base Isolation Layer
著者(和文)	趙桐, 佐藤大樹, 銭曉鑫
Authors(English)	Tong ZHAO, Daiki SATO, Xiaoxin QIAN
出典 / Citation	日本建築学会関東支部研究報告集, , , pp. 449-452
Citation(English)	, , , pp. 449-452
発行日 / Pub. date	2023, 2
権利情報	一般社団法人 日本建築学会

Effects of Wind Characteristics on Residual Drift of the Base Isolation Layer

構造－振動

正会員 ○ 趙 桐^{*1} 正会員 佐藤大樹^{*2}
〃 錢 曉鑫^{*3}

Base-isolated tall building, Base isolation layer, Residual drift
Variation of wind speed and direction

1. INTRODUCTION

The number of base-isolated tall buildings has increased in recent years^[1]. As building height increases, the wind force that acts on building also increases. If the steel dampers are in the base isolation layer, it is possible that residual drift of base isolation layer occurs due to plasticization of the steel dampers. So as to ensure the performance against earthquakes after typhoons, the evaluation of residual drift caused by typhoons is important. Guidelines for the Wind-resistant Design of Seismically Base-isolated Buildings^[2] shows the simplified evaluation method for residual drift based on the maximum deformation. In addition, it is common to evaluate response using the 10-minute wind force that the wind direction and wind speed fixed in wind resistant design^[2], but it cannot take the occurrence of the wind force in the opposite direction to the deformation of base isolation layer.

Therefore, in this paper, the effects of wind speed and direction variation of residual drift at base isolation layer of base-isolated tall building are analyzed based on the results of time history wind-induced response analysis.

2. OUTLINE OF THE MODEL

The outline of analytic model is shown in Fig. 1 and the parameters are shown in Table 1. It is an elasto-plastic 11-DOF model^[3] equivalent to the steel structure building. The time history wind response analysis is conducted in the x and y direction independently without considering torsional vibration.

The stiffness of i^{th} story ${}_u k_i$ ^[4] is determined by Eq (1) considering that the first mode is a straight line.

$${}_u k_i = \frac{{}_u s \omega^2 \cdot {}_u m_i \cdot {}_u s \varphi_i + {}_u k_{i+1}({}_u s \varphi_{i+1} - {}_u s \varphi_i)}{{}_u s \varphi_i - {}_u s \varphi_{i-1}} \tag{1}$$

Where, ${}_u s \omega$: s^{th} mode circular frequency of upper structure, ${}_u m_i$: mass of the i^{th} story of the upper structure, ${}_u s \varphi_i$: s^{th} mode vector of the i^{th} story of upper structure. However, ${}_u k_{11} = 0$, ${}_u s \varphi_0 = 0$.

Fig. 1 shows the restoring force characteristics of dampers,

isolators, and base isolation layer. Time-dependent deformation and repeated deformation dependency are not considered for the restoring characteristics of base isolation layer. The parameters of base isolation layer are determined by Eq. (2) ~ (4).

$$Q_{dy} = W \cdot \alpha_{dy} \tag{2}$$

$$k_{d1} = Q_{dy} / \delta_{dy} \tag{3}$$

$$k_f = 4\pi^2 W / (T_b^2 \cdot g) \tag{4}$$

Where, Q_{dy} , α_{dy} , k_{d1} , δ_{dy} : yield force, shear coefficient, primary stiffness and yield strain of damper; k_f : primary stiffness of isolator; W : weight of the building.

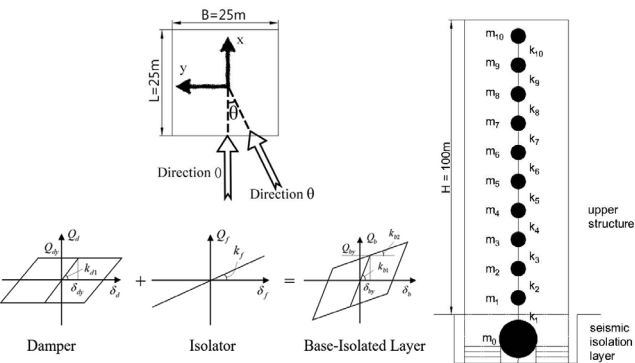


Fig. 1 Outline of the analytical model

Table. 1 Parameter of the analytical model

Aspect ratio (Ar)		4
Height (H)		100 m
Width (B)		25 m
Depth (L)		25 m
Upper Structure	Density (ρ_u)	180 kg/m ³
	Damping ratio (ζ_u)	0.01
	Natural period (T_u)	2.5 s
Seismic Isolation Layer	Yield strain ($\delta_{by}=\delta_{dy}$)	2.5 cm
	Natural period (T_b)	5.0 s
	Shear coefficient of damper (α_{dy})	0.03
	Areal density (ρ_b)	3644 kg/ m ²

3. OUTLINE OF WIND FORCE

There are 2 kinds of wind force used in this paper.

The first one is 10_000, which means 10-minute wind force on a fixed direction and fixed wind speed $U_{H,max} = 50.41$ m/s (height of 100 m, roughness classification of III and return period of 500 years). For the wind force of the upper structure, 10-wave wind force time history waveform is created based on the wind tunnel experiment^[5]. And the wind force of the base isolation layer is 0. As shown in Fig.2, 50s envelope is placed before and after all wind waves respectively to avoid transient responses in the analysis.

The second one is T_000^[6], 10 typhoons (Sample 1~10) with different changes in wind speed and direction are used in this paper. The duration of Sample 1 is shortest in 9 hours and 10 minutes, and that of Sample 9&10 are longest in 40 hours and 10 minutes. As shown in Fig.3(a), the average wind speed at the top of the building varies at intervals of 10 minutes, and the maximum is also 50.41 m/s. However, Sample 6, 8, 9 have two wind speed peaks. The changes of wind direction are shown in Fig.3(b). The wind direction obtained from the typhoon simulation^[6] per 10 minutes. After that, the wind direction is fixed at maximum wind speed to 0° . Wind direction 0° represents the angle facing the building width B as shown in Fig.1. The maximum wind speed of both 10_000 and T_000 is 50.41 m/s. And the wind direction of the maximum wind speed is 0° .

Fig. 4 shows two examples of wind speed and direction of Sample 2 and 8. Fig.5 shows an example of the time history waveform on 10F (Sample 8, Wave 1).

Here, the purpose of setting T_000 is to make the wind condition closer to the actual. To judge whether 10_000 is overestimated compared to T_000.

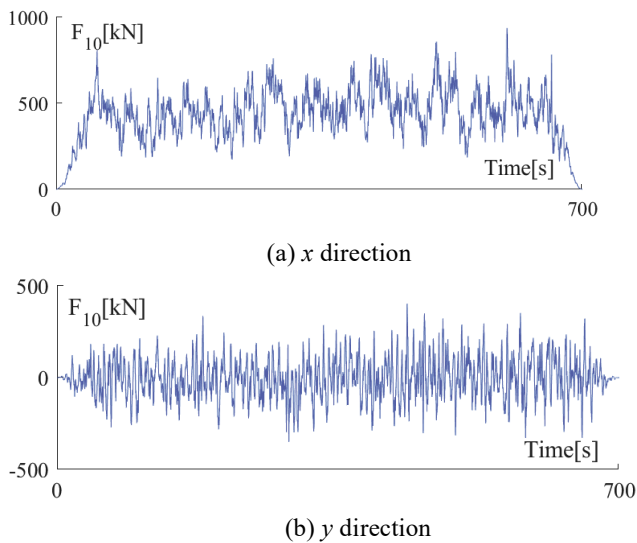


Fig.2 Wind force on 10F (10_000)

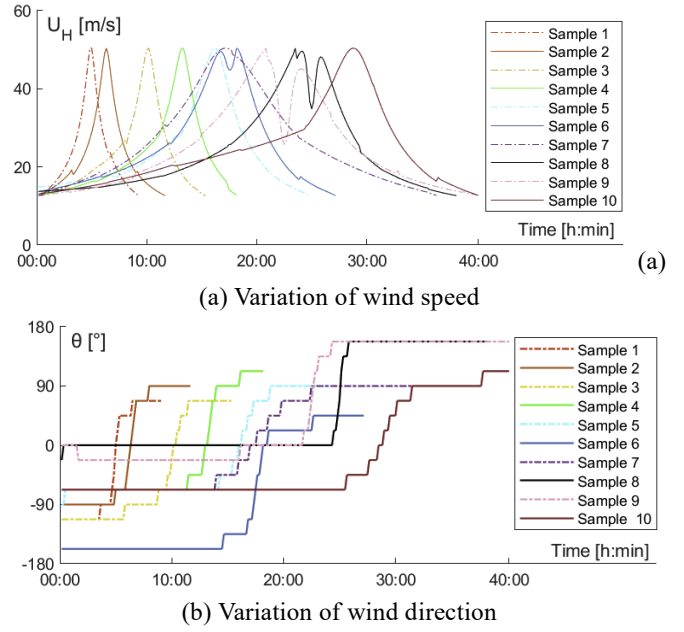


Fig.3 Wind characteristics

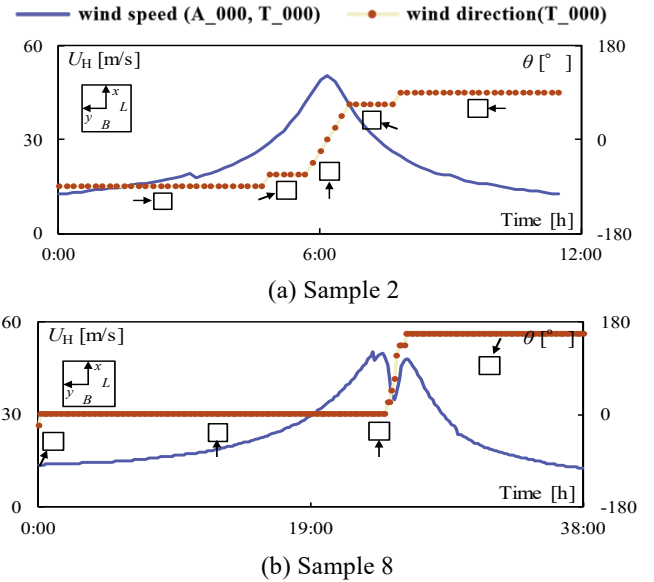


Fig.4 Example of wind speed and direction

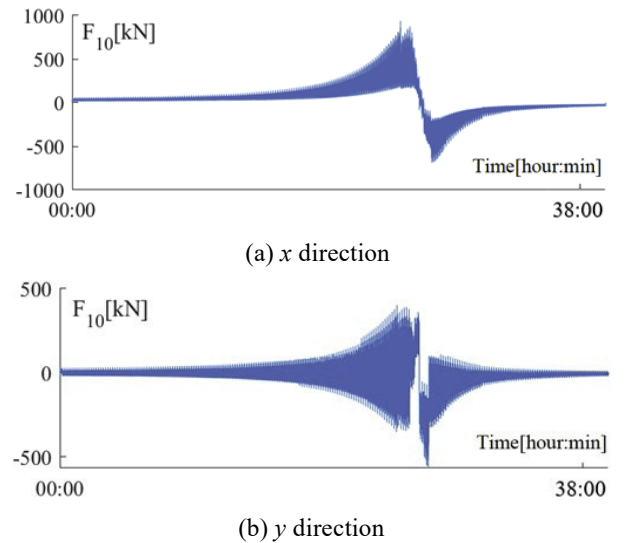


Fig.5 Wind force on 10F (Sample 8, T_000)

4. EVALUATION OF RESIDUAL DRIFT

4.1 Effect of wind speed and direction variation on residual drift

Fig. 6 shows the ensemble by 10 waves average and the standard deviation of the residual drift of base isolation layer $|\delta_{br}|$ (absolute value) for 10 waves.

In the x direction shown in Fig. 6(a) comparing by 10_000 and T_000 for each typhoon sample, in Sample 2, 4, 5, 7, 10, the mean residual drift of base isolation layer of 10_000 is much larger than that of T_000.

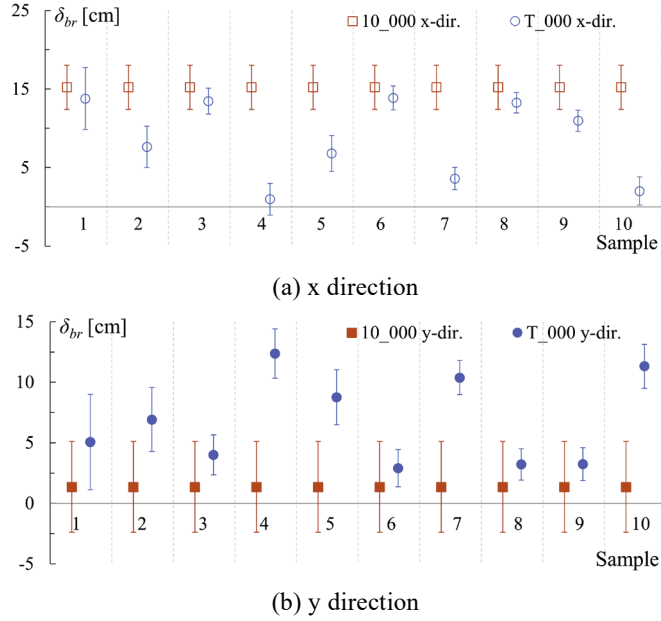


Fig.6 Residual drift of base isolation layer

× Maximum deformation ▲ Residual drift ▲ Eq (5)

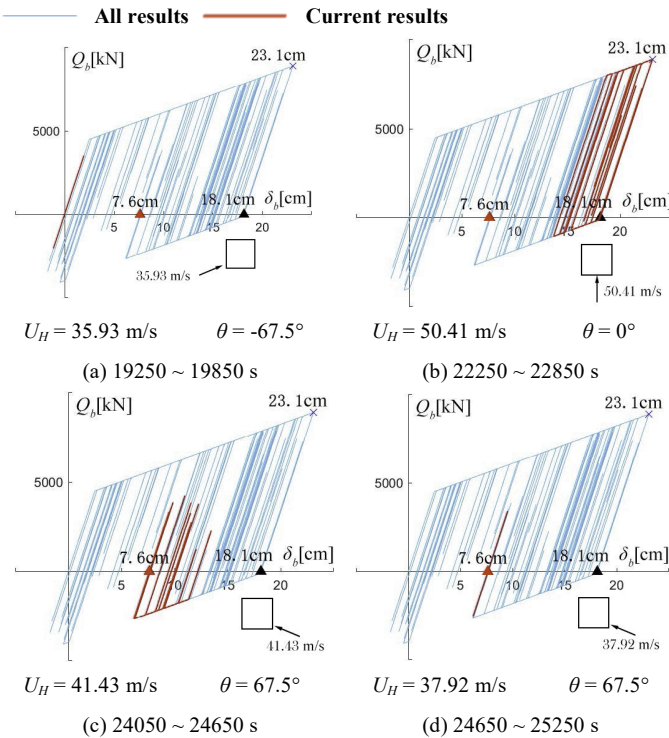


Fig.7 Loop of isolation layer (x-direction, T_000, Sample 2, Wave 1)

But the value of 10_000 for other samples are slightly larger than T_000. In other words, 10_000 has larger residual drift in x direction than T_000 ($T_{000} \leq 10_{000}$) and the evaluation is on the safe side. It is found that T_000 in Sample 2, 4, 5, 7, 10 is overestimated. Therefore, it is useful to

× Maximum deformation ▲ Residual drift ▲ Eq (5)

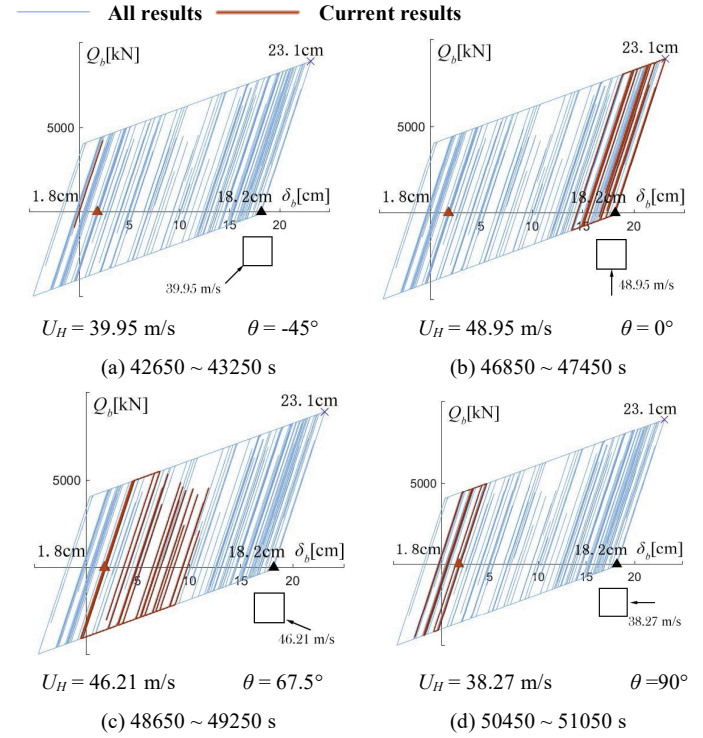


Fig.8 Loop of isolation layer (x-direction, T_000, Sample 4, Wave 1)

× Maximum deformation ▲ Residual drift ▲ Eq (5)

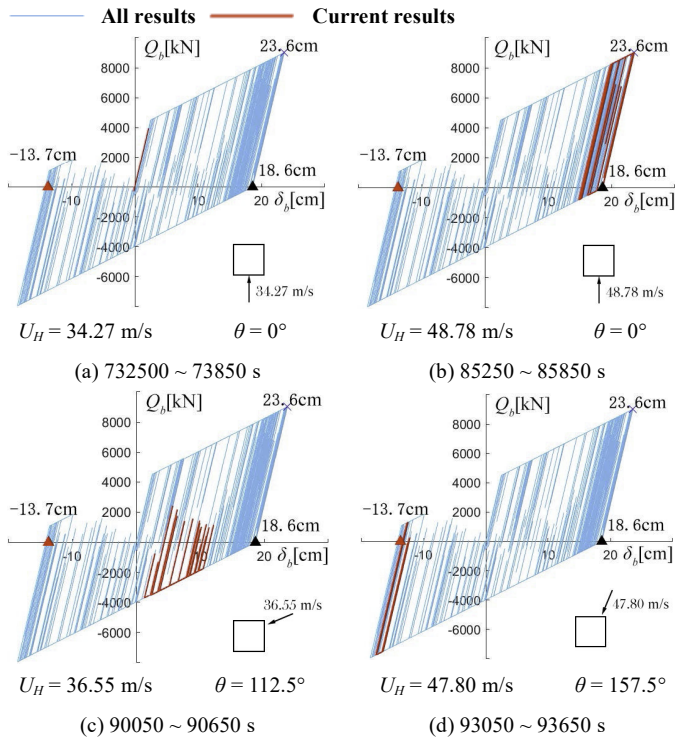


Fig.9 Loop of isolation layer (x-direction, T_000, Sample 8, Wave 1)

consider the wind direction change in the evaluation of the residual drift of the base isolation layer.

On the other hand, it can be seen that the residual drift of the base isolation layer in y direction shown in Fig. 6(b) is relatively smaller than that in x direction in Fig. 6(a). Thus, the discussion in y direction will not be discussed here.

4.2 Simplified evaluation method for residual drift

Fig. 7~9 show the hysteresis loop of base isolation layer of Sample 2, 4 and 8. The black triangle is presumed residual drift calculated by Eq.(5) which is from Guidelines for the Wind-resistant Design^[2] (Simplified evaluation method: the point where the load becomes 0 with primary stiffness from maximum response)

$${}_p\delta_{br} = \frac{\delta_{bmax}(k_{b1} - k_{b2}) + \delta_{by}(k_{b2} - k_{b1})}{k_{b1}} \quad (5)$$

Where, δ_{bmax} : maximum deformation of base isolation layer; k_{b1} , k_{b2} : primary and post-yield stiffness base isolation layer.

(The maximum shear force is less than 2 times the yield force.)

For 10 minutes (red line of Current result) in Fig.7~9 (a), wind force is small, so the vibration of base isolation layer is still within the elastic range. Then, for 10 minutes in Fig.7~9 (b), the base isolation layer becomes plastic due to the increased wind speed, and maximum deformation δ_{bmax} occurs. After that, for 10 minutes in Fig.7~9 (c), the wind speed decreased and began to deform towards opposite direction. For 10 minutes in Fig.7~9 (d), the wind force in the direction opposite to the maximum deformation becomes small, so the base isolation layer vibrates within the elastic range, and finally residual drift δ_{br} occurs.

The ensemble average of presumed residual drift ${}_p\delta_{br}$ for 10-waves comparing with that of residual drift from analysis δ_{br} is shown in Fig.10. Different sample has different degree of rebound effect (on safety side). It can be found that the greater the wind force opposite to the maximum deformation, the more likely the rebound effect will occur.

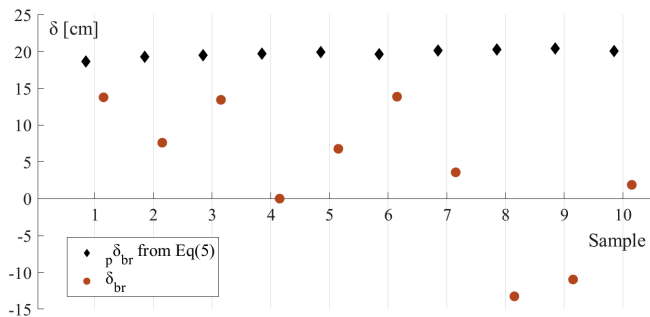


Fig.10 Comparison of δ_{br} VS ${}_p\delta_{br}$

5. Conclusions

*1 *3 東京工業大学 環境・社会理工学院 大学院生

*2 東京工業大学 准教授・博士 (工学)

In this paper, the residual drift of base isolation layer by 10-minute wind force (10_000: 10-minute wind force with constant wind speed and direction used for wind resistance design.) and 10 Samples of typhoon simulation (T_000: Typhoons with variation in wind speed and direction) were compared using a 11DOF model according to a base-isolated tall building. The following conclusions can be drawn:

(1) According to $T_{000} \leq 10_{000}$, even though it is possible that 10_000 would overestimate T_000 on residual drift of base isolation layer, the evaluation is always on the safety side. And it is still effective to consider wind direction variation when evaluating the residual drift.

(2) Due to the wind force acting against the maximum deformation, there will be a rebound effect that the residual drift will vary into the oppsite direction to the presumed residual drift from the simplified evaluation method. This effect is related to the wind speed in the direction opposite to the maximum deformation. As the reverse wind speed increases, the residual drift will decrease. However, when the residual drift decreases to the opposite direction to maximum deformation, it will increase with the increase of the reverse wind force. Simplified evaluation method is safe, but may increase costs when overestimated.

References

- [1] 日本免震構造協会, 2021 年度免震制振データ集積結果, <https://www.jssi.or.jp/wp/wp-content/uploads/2022/12/2021-datasyuseki.pdf>
- [2] 日本免震構造協会, 免震建築物の耐風設計指針, pp. 115-117, 2012.9
- [3] 銭曉鑫, 佐藤大樹, 台風シミュレーションに基づく免震層の残留変形評価, 第 66 回構造工学シンポジウム, 構造工学論文集, 日本建築学会, Vol. 66B, pp. 323-329, 2020.3
- [4] 佐藤大樹, 笠井和彦, 田村哲郎, 粘弾性ダンパーの振幅依存性が風応答に与える影響, 日本建築学会構造系論文集, 第 635 号, pp. 75-82, 2009.1
- [5] 丸川比佐夫, 大熊武司, 北村春幸, 吉江慶祐, 鶴見俊雄, 佐藤大樹, 風洞実験に基づく高層建物の多層層風力によるエネルギー入力性状 (その 2 矩形高層建築物に作用する層風力特性), 日本建築学会学術講演梗概集, B-1, pp. 193-194, 2010.7
- [6] 団栗直希, 西嶋一欽, 確率台風モデルに基づくハザード適合最尤台風の決定方法, 平成 29 年度京都大学防災研究所研究講演発表会, B19, 2018.3

* Graduate Student, Tokyo Institute of Technology *¹

* Associate Professor, FIRST, Tokyo Institute of Technology, Dr. Eng. *²

* Graduate Student, Tokyo Institute of Technology *³